AIP | Physics of Fluids

Large-scale eddies and their role in entrainment in turbulent jets and wakes

Jimmy Philip and Ivan Marusic

Citation: Phys. Fluids **24**, 055108 (2012); doi: 10.1063/1.4719156
View online: http://dx.doi.org/10.1063/1.4719156
View Table of Contents: http://pof.aip.org/resource/1/PHFLE6/v24/i5
Published by the American Institute of Physics.

PHYSICS OF FLUIDS **24**, 055108 (2012)

Large-scale eddies and their role in entrainment in turbulent jets and wakes

Jimmy Philip[a] and Ivan Marusic[b]
Department of Mechanical Engineering, University of Melbourne, VIC 3010, Australia

(Received 16 January 2012; accepted 20 April 2012; published online 18 May 2012)

A large-scale or energy-containing eddy model of turbulent axisymmetric jets and wakes is developed, wherein eddies are randomly distributed in the azimuthal and convecting in the axial directions. The mean velocities and second order statistics obtained from the models agree well with the various available experimental data. There is an average inflow into the turbulent jet at the boundary, which is virtually non-existent for wakes. These eddy contributions are used to reconsider the entrainment process, which has to date been largely conceived as either an "engulfment" or "nibbling" process. Here we suggest that entrainment in turbulent jets be viewed as a three-part-process wherein non-turbulent fluid is "induced" and "engulfed" into the turbulent core due to large-scale eddies, which is converted into turbulent motion by the action of small-scale eddies via "nibbling." However, in wakes there is no induced flow and the primary cause of entrainment is envisaged to be large-scale "engulfment" combined with small-scale "nibbling." © *2012 American Institute of Physics*. [http://dx.doi.org/10.1063/1.4719156]

I. INTRODUCTION

The discovery of coherent structures in turbulent wall bounded[1] and free shear flows[2] has shifted the way one thinks about turbulence in general. Over the past few decades a structural point of view has emerged, wherein turbulent flow can be considered as a collection of organized motion in a *sea* of unorganized motion. Such a description of turbulent motion was originally championed by Townsend[3–5] who described the coherent eddies from two-point correlations (e.g., Grant[6]) before the flow visualization made it self-evident. The photographs of coherent motion in axisymmetric jets[7,8] and wakes[9] are so startling that one is compelled to question: how important are these flow structures in the description of turbulence? For a more precise definition of eddies, organized motions or coherent structures, one is referred to Marusic and Adrian.[10] It is the intent of this article to show that a random collection of coherent large-scale eddies is sufficient for the description of mean and second order statistics in axisymmetric jets and wakes, following the investigations in turbulent boundary layers,[11] co-flowing jets[12] and pressure gradient turbulent boundary layers.[13] This is the first objective.

Given the premise that large-scale eddies provide a fair description of the first and second order statistics, next, their role in "entrainment" is questioned, and this relates to the second objective. Though it was "believed" in the past that large-scale eddies play a major role in the entrainment of non-turbulent (NT) fluid into the turbulent (T) core (see, for example, Liepmann and Gharib[8] for the near field development of a jet and Yoda *et al.*[14] for the far field development and the evolution of large-scale vortices from a simultaneous pair of $n = \pm 1$ helices, where n is the azimuthal wavenumber), recent investigations[15–17] (for a turbulent jet) seem to cast a serious doubt on this viewpoint. To quote from the Introduction of a recent article,[18] "Concerning the physical processes responsible by the entrainment, recent works suggest that the entrainment is mainly caused by

[a]Electronic mail: jimmyp@unimelb.edu.au.
[b]Electronic mail: imarusic@unimelb.edu.au.

small-scale (nibbling) eddy motions acting on the T/NT interface (Westerweel *et al.*, 2005[16]), as proposed originally by Corrsin and Kistler (1955).[19] Specifically Westerweel *et al.* (2005, 2009)[16,17] showed that the engulfment motion caused by the large-scale vortices is not the dominant process for the turbulent entrainment of irrotational fluid in a jet, in agreement with Mathew and Basu (2002).[15] Instead, it is suggested that small-scale 'nibbling' eddy motions may be the dominating entrainment mechanism." The second objective here is, however, to show that large-scale eddies do have a role to play in the entrainment process. Nibbling eddies themselves are important for the more general problem of interface dynamics, and there has been a growing interest over the past decade that is well elucidated in a recent review by Hunt *et al.*[20] Experiments[17,21,22] in sink with direct numerical simulations[18,22–24] have provided valuable information about the vorticity dynamics close to the interface, which in turn is hoped to clarify the entrainment process. Specifically, in the simulations of a far field wake large-scale movements or engulfing motions at the interface are found to be dominated by the inviscid dynamics,[23] and even in jets the large-scale vortical structures are the ones that define the geometrical characteristics of the interface due to their larger radius and longer lifetime.[24] The interface thickness (or the length scale of the vorticity layer, $\delta_\omega(\nu, S)$, where ν and S are viscosity and strain-rate, respectively) in jets scales with Taylor's micro-scale λ because S scales with L_{11}, the integral length scale, due to the large-scale structures; unlike in the oscillating-grid-experiments,[22] where $\delta_\omega \sim \eta$, due to the small-scale "intense-vortical structures"[24] which cause S to scale with λ. The oscillating-grid-experiments have a unique feature – the absence for large-scale motions ($S \sim \lambda$), in contrast to the present model of jets and wakes where only the large-scale motions are considered (of the $\mathcal{O}(L_{11})$).

The process of entrainment is further complicated by the fact that it is easier to think in a "Lagrangian" description wherein the packets of irrotational fluid make their way into the turbulent core across the interface boundary and the visualization or the experimental data is "instantaneous," whereas the data is collected in an "Eulerian" system and mathematically "time-averaged" flow fields are more tractable. In the present work we do not intend to solve the full "entrainment problem" which might need a very detailed representation of the flow field as well as the interface between the turbulent and non-turbulent regions. Instead, with the simple eddy model our intention is primarily to show the relevance of the energy containing eddies in the entrainment process without any precise description of the T/NT interface. Sec. II describes the large eddy model for jets and wakes along with the comparison to some published experimental results, followed by Sec. III wherein their role in entrainment and the problems associated with a good description of entrainment are addressed. Some discussion is presented in Sec. IV, and finally summary and conclusions are given in Sec. V.

II. LARGE-SCALE EDDY MODEL OF AXISYMMETRIC TURBULENT JETS AND WAKES

The axisymmetric jet is modeled by an eddy that is similar to that developed by Nickels and Perry[12] for a co-flowing jet, akin to the double-roller eddy structure suggested by Townsend[3] based on the correlation measurements, and is similar to the structures observed in experiments, for example, by Liepmann and Gharib.[8] Figure 1(a) illustrates such a vortex structure for an axisymmetric jet (comprising of various vortex "rods") and it is envisaged that an array of such vortices are arranged randomly in the azimuthal direction and convecting past an axial location randomly. It should be mentioned that a random collection of "eddies" does not imply that two points in space are uncorrelated, unlike a random collection of "points." The eddy ensures that a specific correlation exists between two points in space characteristic of the turbulent flow. Furthermore, a single eddy type is chosen to represent the jet and wake structures, acknowledging that there is excellent mixing in these flows characterized by a constant eddy viscosity. This is in contrast to wall bounded flows where a hierarchy of eddies[11,13] is required to represent the flow characterized by eddy viscosity varying in the wall-normal direction. Streamwise, azimuthal, and radial directions are indicated by x, θ, and r, and the corresponding velocities by U_x, U_θ, and U_r. The r-θ plane is the same as y-z plane in Figure 1. The coordinates are normalized by the characteristic length scale Δ, such that,

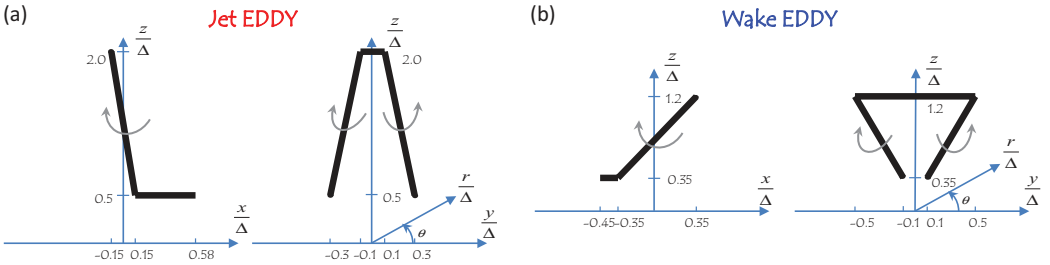

FIG. 1. Two views of the eddy structure used in the model. (a) Jet. (b) Wake. The curved arrows show the direction of the induced velocity due to the vortex-rod-structures constituting the eddy. These eddy models have similarities to the large-scale structures observed in Figures 6 and 7 for turbulent flows.

$\Delta^2 = \int_0^\infty r^2 \langle U_x \rangle \, \mathrm{d}r / \int_0^\infty \langle U_x \rangle \, \mathrm{d}r$, in accordance with Nickels and Perry[12] and Townsend,[3] where $\langle\,\rangle$ denotes averaged quantity.

The calculation procedure is described for the axisymmetric jet eddy, cf. Figure 1(a) (and the procedure for the wake follows in a similar fashion). The five vortex-rods are prescribed with a Gaussian vorticity distribution and a constant circulation. The velocity field, $\mathbf{v}(x, y, z)$, associated with all five rods of a single eddy is calculated using the Biot-Savart law on a three-dimensional cartesian grid. Thereafter, the power spectral density ($p_{ij}(k_1\Delta, y, z)$, where k_1 is the axial wavenumber and, i and j go from 1 to 3 corresponding to the velocity components) is found using standard FFT routines in the axial (x) direction. To account for the intermittency, the spectral density field is "jittered" (or convolved) using a Gaussian kernel in the y-z plane, followed by the second order tensorial transformation to r-θ coordinate system, $q_{ij}(k_1\Delta, r, \theta)$. Averaging in the axial and azimuthal directions results in distribution of all the stresses in the radial direction, $\overline{q}_{ij}(r)$ (for example, $\overline{u_x^2}(r)$, $\overline{u_x u_r}(r)$, etc.). The axial mean velocity can be obtained similarly by averaging $\mathbf{v}(x, y, z)$ in the axial direction ($U(y, z)$), followed by "jittering" and a transformation to r-θ system ($U(r, \theta)$) and finally averaging in the azimuthal direction ($U(r)$). The above calculation is performed for a single eddy. It is envisaged that a random distribution of such eddies is distributed along the azimuthal direction and a constant density of such eddies passes a fixed axial location. Instead of physically distributing the eddies randomly and calculating the velocity field, one can resort to Campbell's theorem[25] for shot-noise process. For an uncorrelated random distribution of eddies, Campbell's theorem shows that when the number density of eddies is fixed, the mean velocity field and variance (or root-mean-square) distribution from the random collection of eddies can be found from just a single eddy multiplied by the eddy-density. The free parameter is the eddy-density, which is arbitrarily fixed by making the value of axial stress ($\overline{u_x^2}$ in Figure 3 below) to approximately match with the experimental ones at the centerline. Further details of the calculation procedure can be found in Nickels and Perry[12] and Nickels and Marusic.[26]

A similar model is proposed for turbulent wakes in Figure 1(b) where the defect profile is modeled which also corresponds to the change in the vortex-rod direction in the x-z plane. Here the characteristic length scale $\Delta := r_{1/2}$, where $r_{1/2}$ is the the location where defect-velocity falls to half its maximum value, consistent with the usual self-similar analysis of axisymmetric wakes (e.g., Pope[27]).

Figure 2 shows the comparison of mean velocity profiles for jets and defect-profiles for wakes with various published experimental results (indicated in the figure), where $f := \langle U_x \rangle / U_c$ and $(U_\infty - \langle U_x \rangle)/U_c$ for jets and wakes, respectively, and U_c the characteristic or centerline velocity in jets/wakes (which is a function of x) and U_∞ the free-stream velocity in wakes. Turbulent stresses are compared in Figure 3(a) for jets and in Figure 3(b) for wakes. The experimental symbols are consistent with those in Figure 2. It is noted that even though lots of experimental data for axisymmetric turbulent jets are available, there is an acute scarcity of the same in wakes where all the components of velocity are measured at a sufficiently large x/Δ such that self-similarity is established.

Considering simple vortex-rods are employed, there is a good agreement between the model and the experimental results. Out of the five vortex-rods the most important are the two vertical ones

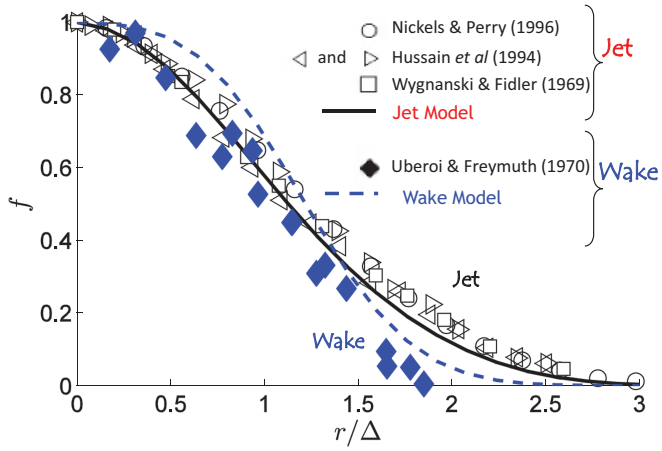

FIG. 2. Mean velocity profiles for jets and wakes. Full line is from the jet model calculations whereas broken line corresponds to wake. Empty symbols represent various jet experiments, ○ Nickels and Perry,[26] ◁ and ▷ Hussein *et al.*,[28] □ Wygnanski and Fiedler,[29] and filled symbols (◆) are the wake experiments of Uberoi and Freymuth.[30] Note that for the experiments of co-flowing jets by Nickels and Perry,[26] the free stream velocity is subtracted from the axial velocity.

in the y-z plane of Figure 1 – the double-roller eddy structure, which alone could give the correct shape of the experimental stress profiles of Figure 3. The main function of the other three vortex-rods (which are consistent with the flow visualization) is to provide correct stress ratios. An important difference between the stress profiles for jets and wakes is that azimuthal stress is higher than radial stress in jets whereas the opposite is true in wakes. The model accomplishes this by an increased tilt of the double-roller in the x-z plane of Figure 1(b), with respect to the z axis. As the double-roller becomes more and more vertical the azimuthal stress increases in comparison to the radial stress, which is evident when the velocity field associated with them is observed. It should be mentioned that even though a fixed shape of the eddy model is presented in Figure 1 its precise shape is of lesser importance. However, the particular shape of the eddy employed here with its random distribution is found to closely predict the experimental stress profiles for the known parameters of the jets/wakes. As mentioned above, the location of the different vortex-rods are of a greater influence in generating correct stresses.

It is emphasized that the model takes into account only the large scales of motion or energy containing eddies as the spectra in Figure 4(a) show. The axial wavenumber and spectra are denoted by k_1 and Φ_{11}, respectively. The model (in broken lines) at different radial locations are compared with the experiments by Nickels and Perry[12] (in solid lines). The model-spectra falls off at a lower

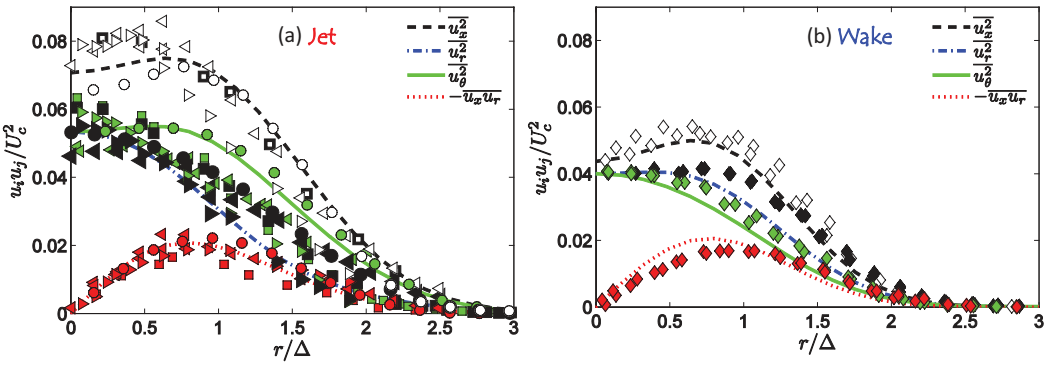

FIG. 3. Turbulent stress profile for jets and wakes. (a) Jet. (b) Wake. Lines are the calculations from the model and symbols are experimental points corresponding to Figure 2. Different shades (color) represent different stresses. As an example, for the jet data of Nickels and Perry,[26] the shaded (colored) symbols are: ○ u_x^2, (black circles) u_r^2, (green circles) u_θ^2, (red circles) $-u_x u_r$.

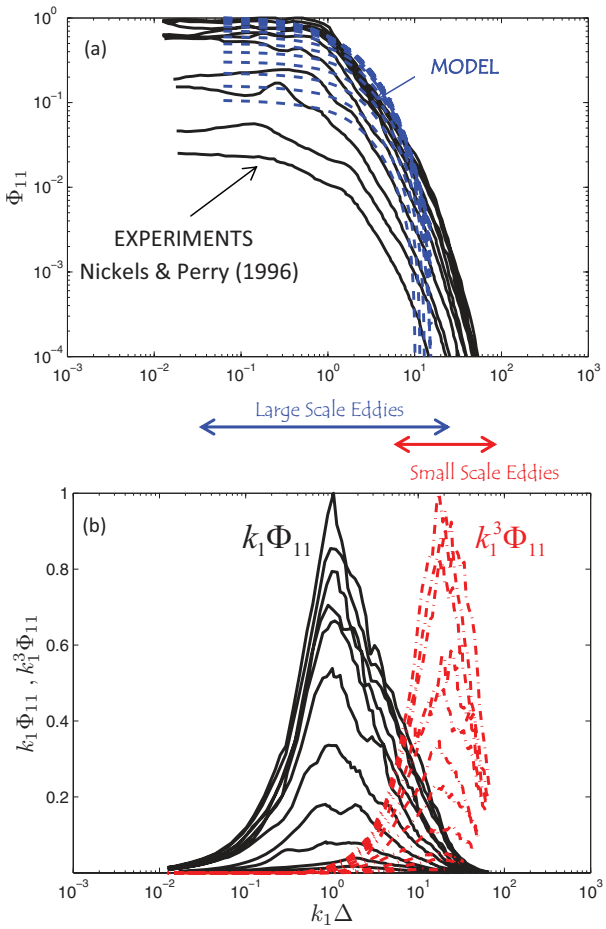

FIG. 4. Normalized spectra of an axisymmetric jet at various radial poistions. (a) Comparison of model in broken (blue) lines with experiments of Nickels and Perry[26] in full (black) lines. (b) Pre-multiplied spectra ($k_1\Phi_{11}$) of the experimental data from (a) in full (black) lines and dissipation spectra ($k_1^3\Phi_{11}$) in dashed-dotted (red) lines.

wavenumber, as expected, indicating the neglect of small-scale motion. The pre-multiplied spectra in Figure 4(b) ($k_1\Phi_{11}$, the area under which represents energy) from the data of Nickels and Perry[12] (in solid line) and the same data in $k_1^3\Phi_{11}$ form (dash-doted line), representing dissipative small scales, which again show the scale separation that is inherent in a resolved experimental data, is absent from the model. It is well known that turbulent flow contains a range of scales. Assuming Fourier wavenumbers to represent scales, it can be observed that the eddy-model produces a broadband spectra unlike models which are confined in spectral space. This possibility exists only in jets and wakes where the eddy almost fills the entire flow, in contrast to wall bounded flows where a hierarchy of scales is needed. It is important to mention the limitation of the present model, which is restricted to the investigations of only up to second order statistics. At present, it is not completely clear how higher order statistics from the model will compare with the actual flow, and a fair description of these statistics might even involve going beyond the simplified model of turbulent jets and wakes involving a single representative eddy, as the one developed here.

III. ROLE OF LARGE-SCALE EDDIES IN ENTRAINMENT

The model developed above corresponds to a statistically steady self-similar condition, and it is instructive to look at the flow that is drawn into the jet core radially. This is the average entrained fluid. Using the axial mean flow calculated from the model (cf. Figure 2), and for a self-similar

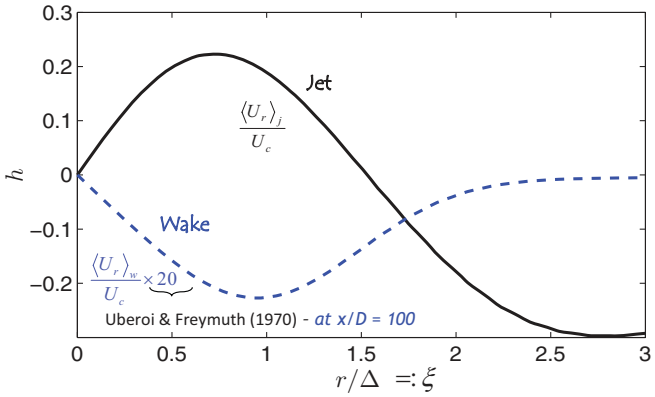

FIG. 5. Radial velocity profiles from the model for jet and wake (using continuity equation).

turbulent jet/wake, radial velocity is calculated using the continuity equation. Specifically, for the axisymmetric jet, with $\Delta \propto x^1$ and $U_c \propto x^{-1}$, the continuity equation reduces to $(h\xi)' = \xi(f\xi)'$, where $h := \langle U_r \rangle / U_c$ is the normalized jet radial velocity, $\xi := r/\Delta$ and prime ($'$) denotes differentiation with respect to ξ (e.g., Pope[27]). The distribution of h with ξ is plotted in Figure 5 with a solid line, showing a definite inflow at the boundary into the jet core. For axisymmetric wakes only partial similarity exists; with $\Delta \propto x^{1/3}$ and $U_c \propto x^{-2/3}$ continuity equation reduces to $(h_w\xi)' = -\xi(2/3 f + 1/3 f'\xi)$, where $h_w := \langle U_r \rangle C_{expt} / U_c^2$ is the normalized wake radial velocity, which unlike for jets depends on an experimental constant, $C_{expt}(x)$. Also shown in Figure 5 is $h := \langle U_r \rangle / U_c \times 20$ for the wake, where the numerical value corresponds to the experiments of Uberoi and Freymuth[30] at $x/D = 100$ and D the sphere diameter behind which the wake is generated. A good approximation to the mean velocity profiles for jets and wakes are $f = 1/(1 + a\xi^2)^2$ and $\exp(-b\xi^2)$, respectively, where a and b are constants (e.g., Townsend[3] and Pope[27]). Integration using the continuity equation given above results in $h = (1/2)(\xi - a\xi^3)/(1 + a\xi^2)^2$ for jets (Pope[27]) and $h_w = -(1/3)\xi \exp(-b\xi^2)$ for wakes, which are close to the ones calculated in Figure 5 numerically. For wakes the radial velocity magnitudes are much smaller than those for jets and there is hardly any or no inflow at the edge of the wake, in contrast to jets. Fluid in the core seems to be pushed out to some extent due to radial velocity in jets whereas in wakes there is a drawing-in of fluid (likely related to engulfment). Thus, in the "averaged" sense, large-scale eddies can account for the flow which is entrained into the turbulent core. In this regard, it should be noted that even in laminar jets there is an inflow, albeit due to viscous stresses which are much smaller compared to the turbulent stresses, when the jet is turbulent. And since the eddy-model predicts this inflow, the large-scale eddies are seen as a source for it.

The "instantaneous" picture can, however, be slightly different. Considering turbulent jets, Figure 6 shows the caricature of an instantaneous turbulent core (hand drawn to roughly match the visualization by Westerweel *et al.*[17]) and shaded gray. The thick (red) line is the averaged boundary and towards the right hand side is the averaged velocity profile with exaggerated radial velocity. As mentioned above there is an induced motion inwards at the boundary and the fluid is pushed outward from the axis. An approximate instantaneous view is shown between the two vertical (blue) lines, where there is an induced flow towards the boundary of the jet along with the fluid that is engulfed into the core (shown by shaded areas); this is due to the large-scale eddies. Along the boundary smaller eddies nibble the non-turbulent fluid, depicted by (black) circular arrows. Since no non-turbulent fluid packet (in a Lagrangian sense) can become turbulent unless it crosses the boundary, and since at the boundary there is always small-scale eddies nibbling, every fluid packet that becomes turbulent is nibbled. This process is the same as the "small-scale" turbulent diffusion due to momentum transfer. For jets the overall process can be envisaged as: large eddies induce non-turbulent fluid towards the turbulent boundary along with some fluid being engulfed, which is nibbled by the small scales and is made turbulent. Apart from this, small eddies can themselves nibble and move into the non-turbulent fluid; however, since the average boundary in a jet is stationary (for

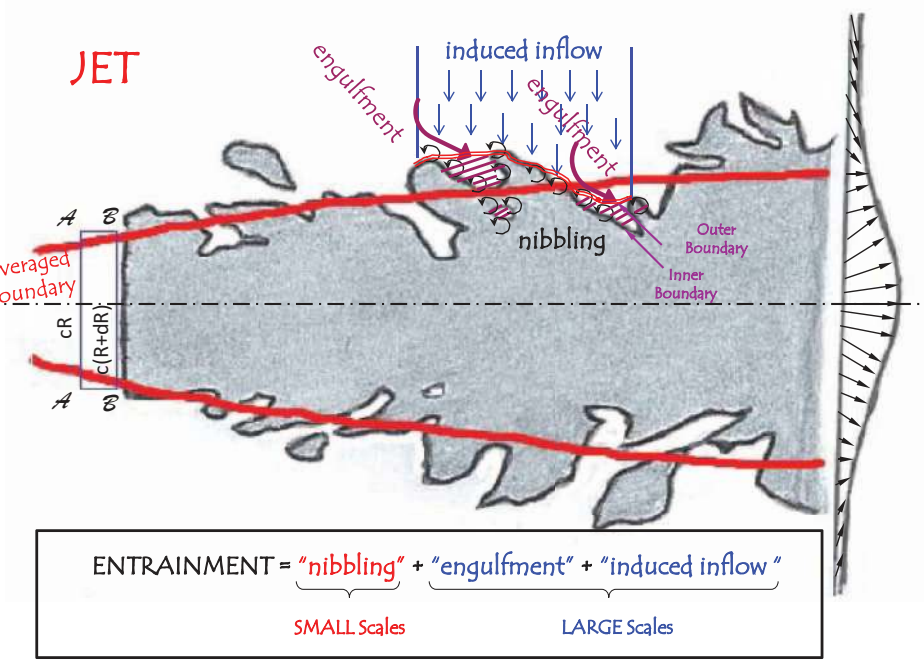

FIG. 6. A caricature of turbulent jet and the entrainment.

a particular x), this is not a very efficient process for making the fluid turbulent. In short, entrainment can be viewed as a three-part-process involving both small scales (for "nibbling") plus large scales (causing "engulfment" and an "induced inward motion").

A similar picture can be sketched for wakes (by observing the flow visualization by Cannon, Champagne, and Glezer[9]), as shown in Figure 7, and here too the averaged velocity vectors are drawn with exaggerated radial velocities. The major variance from jets is that there is negligible induced inward motion due to large-scale eddies at the boundary. Therefore, any entrainment is only due to small-scale nibbling and large-scale engulfment, as shown in the figure between the two vertical (blue) lines. In that sense, to understand the different roles played by small and large scales, the study of wakes might be more profitable as it eliminates one cause of entrainment. In the

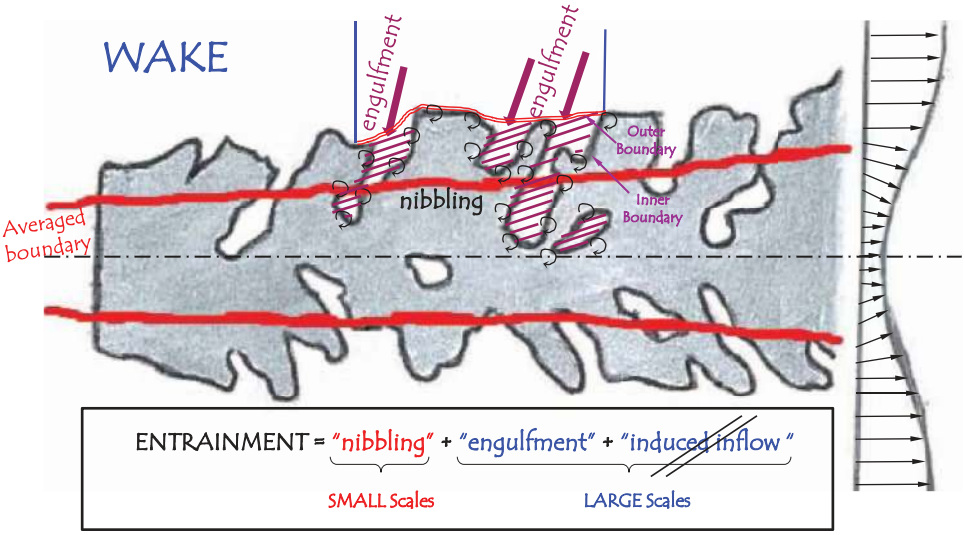

FIG. 7. A caricature of turbulent wake and the entrainment.

description above, the term "engulfed fluid" refers to the shaded areas in Figures 6 and 7, in-between the double (red) line – the "outer boundary" and the black line – the "inner boundary" of the jet. It is more precisely defined by fixing a low and high threshold level, (say 0.1 - outer boundary and 0.9 - inner boundary) of a passive scalar present in the turbulent flow (with scalar value close to 1 inside the turbulent region), and calling the in-between fluid as the engulfed fluid.[15,17,31] Even though this is a good working definition for precisely quantifying the engulfed "scalar" fluid, it has no direct relation to the velocity field (because the equations of velocity are decoupled from that of a passive scalar). In this respect, for the jet flow it is not easy to distinguish between the "engulfment" and "induced inflow" except when a scalar field is present. And this can only be shown symbolically as in Figure 6. Physically engulfed fluid can be thought of as a "local" effect of the large-eddies, wherein the eddies distort the interface and engulf the fluid,[3] whereas the "induced inflow" as a non-local effect wherein the fluid is drawn from far-field. However, in wakes where there is no induced inflow and the large-scale contribution to the entrained fluid can be represented by engulfment. Regarding the caricatures in Figures 6 and 7 it should be mentioned parenthetically that the shaded region is based on flow visualization (of a passive scalar) while the larger arrows (in Figure 6) are induced motion and the smaller curved arrows indicate nibbling vortices at the "edge" of the T/NT interface. However, it is known that pathlines (of velocity) and scalar field from flow visualization could be different,[32,33] so caution is required in interpreting them. Also see the simultaneous visualization and velocity field measurements by Westerweel *et al.*[17]

IV. DISCUSSION

In Sec. III the radial velocity profiles were calculated using continuity employing the axial velocity profiles obtained from the model. However, a simpler method to estimate the average radial velocity at the boundary can be developed following Stewart.[34] Consider the control volume at the left hand side of Figure 6. At section $\mathcal{AA}$, let cR be the characteristic radius of the average jet boundary, where c is a constant and R, the radius ($\propto\Delta$) and kU_c the average velocity, with a constant k. The flow into $\mathcal{AA}$ is $kU_c\pi(cR)^2$. Similarly at section $\mathcal{BB}$, at a distance dx downstream, the outflow is $k(U_c + dU_c)\pi(c(R + dR))^2$, and across $\mathcal{AB}$ is $2\pi c(R + dR)U_r\,dx$. This in turn shows $U_r \propto 1/R\,d(R^2U_c)/dx$ (which is valid for wakes also), and when combined with how R (or Δ) and U_c are varying with x, results $U_r \propto 1/R$ for jets and $U_r = 0$ for wakes at the boundary, as mentioned previously. Similarly for plane jets and wakes, where $\Delta \propto x$, $U_c \propto x^{-1/2}$ and $\Delta \propto x^{1/2}$, $U_c \propto x^{-1/2}$ (e.g., Tennekes and Lumley[35]) respectively, $U_r \propto d(LU_c)/dx$, where $L \propto \Delta$ (and U_r is the velocity normal to the axis). This again shows that even in plane jets there is an averaged velocity at the boundary which is absent in plane wakes, similar to axisymmetric jets and wakes, respectively. It should be mentioned that there is no dearth of evidence for the induced motion into a turbulent jet. For example, the calculation of entrained fluid from the measured velocity profile by Hussain *et al.*[28] match very well with the bulk entrainment measured by Ricou and Spalding[36] or the particle image velocimetry (PIV) measurements of Liepmann and Gharib[8] at a fixed axial position which show the instantaneous radial velocity into the jet core, or, the photographs by Werlé in the book by van Dyke[37] which show explicitly the streamlines of fluid entraining into a turbulent axisymmetric and plane jet. Similar is the case with co-flowing jets where PIV measurements of Han and Mungal[38] at the outside of the main jet confirm the induced flow. Even at extremely high Reynolds numbers Mungal and Hollingsworth[39] as well as Mungal *et al.*[40] have found that the large-scale eddies continue to exist and are no different from those found at the laboratory scale flows, with the same fluid-mechanical picture of entrainment (cf. Figure 11 of Mungal and Hollingsworth[39]).

As an interesting aside, it should be mentioned that jets and wakes cannot be transformed one into another by merely a change in the frame of reference because of the broken Galilean invariance in spatially developing flows or in flows with specific origin.[41] This is also exemplified in the different ways Δ and U_c develop in jets and wakes, as well as the difference in the large-eddy structures. Furthermore, co-flowing jets behave more like regular jets in terms of the induced inflow (e.g., Han and Mungal[38]) than wakes, however, with a difference (cf. Figure 3(a)).

Entrainment has been viewed here as a combination of small-scale nibbling plus a large-scale engulfment and induced inflow. However, another view point would be to think only in terms of

eddies or vortices, with merely a difference in scales. In fact such a scale separation indeed exists in turbulent jets as shown in Figure 4(b) from the experimental data of Nickels and Perry.[12] Most of the energy is contained in scales of order Δ (which corresponds to the model eddies) whereas most of the dissipation is happening at scales which are more than an order of magnitude smaller than Δ (and those are neglected in the model). Thus, it might be more appropriate to refer to the model large-scale eddies as the "energy containing eddies," which cause engulfment and induce inflow, whereas dissipative scale eddies which cause nibbling (with the obvious point that nibbling is only at the boundary), both having the same characteristics except that they operate at different scales. And there is no reason to exclude the possibility that more than two scales (or even a continuum of scales with varying effects) might be involved in the entrainment process. The overall process might even be called "vortex entrainment" – only that vortices of different scales play different roles in the entrainment process.

From an entrainment point of view, wakes are much simpler than jets due to the absence of induced motion, and the active processes being only nibbling and engulfment. However, an even simpler case would be where the process is "pure" nibbling. (A "pure" engulfment or induced inflow is not possible since nibbling is always the final act in the transformation of non-turbulent fluid into turbulent.) Such a case of pure nibbling (though not addressed thus) has indeed been investigated[21,22] wherein an oscillating grid is used to form the turbulent boundary and nibbling is the only reason for entrainment (even though the nibbling eddies are almost as large as the largest scales of the motion). This is one investigation where the role of small-scale eddies can be studied without any influence from large-scale motions, and thus it is not surprising that the stain-rate and the interface thickness scale with λ and η, respectively – the dissipative eddies scales, in contrast to jets and wakes where the inviscid mechanism dominates at scales of L_{11}.

V. SUMMARY AND CONCLUSIONS

It has been shown in the present work that large-scale eddy models, assumed to be randomly distributed in the azimuthal and convecting in the axial directions can be built for turbulent axisymmetric jets and wakes which agree reasonably well with the experimental results in predicting the mean velocity and normal/shear stress profiles. Since they carry most of the energy, they can also be called the energy containing eddies (and because they do not take into account the small dissipative scale motion, as evident from the spectra). This structural view of thinking in terms of large eddies brings at least some order in understanding the otherwise non-coherent disorganized motion. These energy containing eddies draw fluid into the turbulent core, in an averaged sense. Instantaneously, some non-turbulent fluid is induced towards the boundary whereas some of the fluid is engulfed, both of which have to pass through the T/NT interface where it is nibbled by small-scale eddies into a turbulent one. There is also the possibility that small-scale nibbling eddies can themselves reach out into the irrotational regime, transforming non-turbulent fluid into turbulent – akin to a diffusion effect. In jets, entrainment can be viewed as a combined effort of large-scale eddies via engulfing and inducing irrotational fluid, and small-scale eddies via nibbling, whereas in wakes the induced motion is virtually nonexistent and the large-scale contribution is represented by engulfment. In hindsight, from an entrainment perspective, jet flow might seem the most complicated (with effects of engulfment, induced motion and nibbling), whereas wakes much simpler (with only engulfment and nibbling), and the oscillating-grid-experiment the simplest with only nibbling as the dominant mechanism.

ACKNOWLEDGMENTS

The authors wish to thank Professor Ronald J. Adrian for discussions on the entrainment process. The Australian Research Council is gratefully acknowledged for its financial support.

[1] S. J. Kline, W. C. Reynolds, F. A. Schraub, and P. W. Runstadler, "The structure of turbulent boundary layers," J. Fluid Mech. **30**, 741–773 (1967).
[2] G. L. Brown and A. Roshko, "On density effects and large structure in turbulent mixing layers," J. Fluid Mech. **64**, 775–816 (1974).

[3] A. A. Townsend, *The Structure of Turbulent Shear Flow* (Cambridge University Press, 1956).
[4] A. A. Townsend, "The mechanism of entrainment in free turbulent flows," J. Fluid Mech. **26**, 689–715 (1966).
[5] A. A. Townsend, "Organized eddy structures in turbulent flows," PCH, PhysicoChem. Hydrodyn. **8**(1), 23–30 (1987).
[6] H. L. Grant, "The large eddies of turbulent motion," J. Fluid Mech. **4**, 149–190 (1958).
[7] P. E. Dimotakis, R. C. Miake-Lye, and D. A. Papantoniou, "Structure and dynamics of round turbulent jets," Phys. Fluids **26**, 3185–3192 (1983).
[8] D. Liepmann and M. Gharib, "The role of streamwise vorticity in the near-field entrainment of round jets," J. Fluid Mech. **245**, 643–668 (1992).
[9] S. Cannon, E. Champagne, and A. Glezer, "Observations of large-scale structures in wakes behind axisymmetric bodies," Exp. Fluids **14**, 447–450 (1993).
[10] I. Marusic, and R. A. Adrian, "The eddies and scales of wall turbulence," in *Ten Chapters in Turbulence*, edited by P. Davidson, Y. Kaneda, and K. R. Sreenivasan (Cambridge University Press, Cambridge, in press).
[11] A. E. Perry and M. S. Chong, "On the mechanism of wall turbulence," J. Fluid Mech. **119**, 173–217 (1982).
[12] T. B. Nickels and A. E. Perry, "An experimental and theoretical study of the turbulent coflowing jet," J. Fluid Mech. **309**, 157–182 (1996).
[13] I. Marusic and A. E. Perry, "A wall-wake model for the turbulence structure of boundary layers. Part 2. Further experimental support," J. Fluid Mech. **298**, 389–407 (1995).
[14] M. Yoda, L. Hesselink, and M. G. Mungal, "Instantaneous three-dimensional concentration measurements in the self-similar region of a round high-Schmidt-number jet," J. Fluid Mech. **279**, 313–350 (1994).
[15] J. Mathew and A. J. Basu, "Some characteristics of entrainment at a cylindrical turbulence boundary," Phys. Fluids **14**, 2065–2072 (2002).
[16] J. Westerweel, C. Fukushima, J. M. Pedersen, and J. C.R. Hunt, "Mechanics of the turbulent nonturbulent interface of a jet," Phys. Rev. Lett. **95**, 174501 (2005).
[17] J. Westerweel, C. Fukushima, J. M. Pedersen, and J. C.R. Hunt, "Momentum and scalar transport at the turbulent/non-turbulent interface of a jet," J. Fluid Mech. **631**, 199–230 (2009).
[18] C. B. da Silva, R. J.N. dos Reis, and J. C.F. Pereira, "The intense vorticity structures near the turbulent/non-turbulent interface in a jet," J. Fluid Mech. **685**, 165–190 (2011).
[19] S. Corrsin and A. L. Kistler, "Free-stream boundaries of turbulent flows," Technical report, NACA TN-1244, Washington, DC, 1955.
[20] J. C. R. Hunt, I. Eames, C. B. da Silva, and J. Westerweel, "Interfaces and inhomogeneous turbulence," Philos. Trans. R. Soc. London, Ser. A **369**, 811–832 (2011).
[21] M. Holzner, A. Liberzon, M. Guala, A. Tsinober, and W. Kinzelbach, "Generalized detection of a turbulent front generated by an oscillating grid," Exp. Fluids **41**, 711–719 (2006).
[22] M. Holzner, A. Liberzon, N. Nikitin, W. Kinzelbach, and A. Tsinober, "Small-scale aspects of flows in proximity of the turbulent/nonturbulent interface," Phys. Fluids **19**, 071702 (2007).
[23] D. K. Bisset, J. C. R. Hunt, and M. M. Rogers, "The turbulent/non-turbulent interface bounding a far wake," J. Fluid Mech. **451**, 383–410 (2002).
[24] C. B. da Silva and J. C. F. Pereira, "The role of coherent vortices near the turbulent/non-turbulent interface in a planar jet," Philos. Trans. R. Soc. London, Ser. A **369**, 738–753 (2011).
[25] A. Papoulis, *Probablity, Random Variables, and Stochastic Processes* (McGraw-Hill, 1991).
[26] T. B. Nickels and I. Marusic, "On the different contributions of coherent structures to the spectra of a turbulent round jet and a turbulent boundary layer," J. Fluid Mech. **448**, 367–385 (2001).
[27] S. B. Pope, *Turbulent Flows* (Cambridge University Press, 2000).
[28] H. J. Hussein, S. P. Capps, and W. K. George, "Velocity measurements in a high-Reynolds-number, momentum-conserving, axisymmetric, turbulent jet," J. Fluid Mech. **258**, 31–75 (1996).
[29] I. Wygnanski and H. Fiedler, "Some measurements in the self-preserving jet," J. Fluid Mech. **38**, 577–612 (1969).
[30] M. S. Uberoi and P. Freymuth, "Turbulent energy balance and spectra of the axisymmetric wake," Phys. Fluids **13**, 2205–2210 (1970).
[31] N. D. Sandham, M. G. Mungal, J. E. Broadwell, and W. C. Reynolds, "Scalar entrainment in the mixing layer," in *Proceedings of the Summer Program 1988* (Center for Turbulence Research, Stanford University, Stanford, CA, 1988), pp. 69–76.
[32] F. R. Hama, "Streaklines in a perturbed shear flow," Phys. Fluids **5**, 644–650 (1962).
[33] M. G. Mungal, "Large-scale structure in turbulent diffusion flames - evidence, implications, origins," Dev. Chem. Eng. Miner. Process. **7**(3/4), 287–300 (1999).
[34] R. W. Stewart, "Irrotational motion associated with free turbulent flows," J. Fluid Mech. **1**, 593–606 (1956).
[35] H. Tennekes and J. L. Lumley, *A First Course in Turbulence* (The Massachusetts Institute of Technology, 1972).
[36] F. P. Ricou and D. B. Spalding, "Measurements of entrainment by axisymmetrical turbulent jets," J. Fluid Mech. **11**, 21–32 (1961).
[37] M. van Dyke, *An Album of Fluid Motion* (Parabolic, California, 1982).
[38] D. Han and M. G. Mungal, "Direct measurement of entrainment in reacting/nonreacting turbulent jets," Combust. Flame **124**, 370–386 (2001).
[39] M. G. Mungal and D. K. Hollingsworth, "Organized motion at a very high Reynolds number jet," Phys. Fluids A **1**, 1615–1623 (1989).
[40] M. G. Mungal, A. Lozano, and I. van Cruyningen, "Large-scale dynamics in high Reynolds number jets and jet flames," Exp. Fluids **12**, 141–150 (1992).
[41] P. Huerre and P. A. Monkewitz, "Local and global instabilities in spatially developing flows," Annu. Rev. Fluid Mech. **22**, 473–537 (1990).